Electronic Excitations in Carbon Nanostructures: Building-Block Approach

Ralf Hambach[1,3], Christine Giorgetti[1,3], Xochitl Lopez[1,2], and Lucia Reining[1,3].

[1] LSI, Ecole Polytechnique, CNRS, CEA/DSM, Palaiseau, France
[2] University of Texas at San Antonio, United States
[3] European Theoretical Spectroscopy Facility

15. 10. 2010 — ETSF workshop, Berlin

EELS on SWCNTs

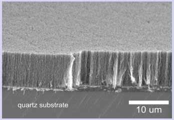

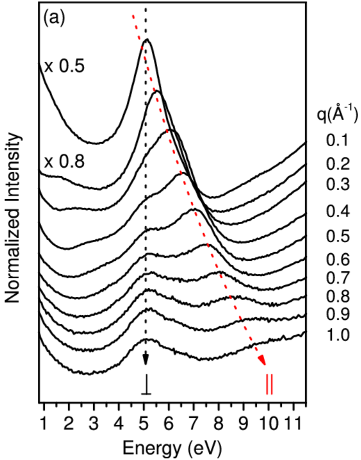

specimen

- oriented SWCNT
- diameter: 2 nm
- nearly isolated

spectroscopy

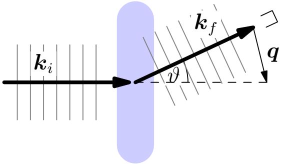

[C. Kramberger, R. H., Ch. Giorgetti, *et.al.*: PRL **101**, 266406 (2008)]

EELS on SWCNTs

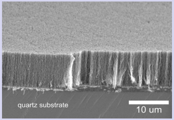

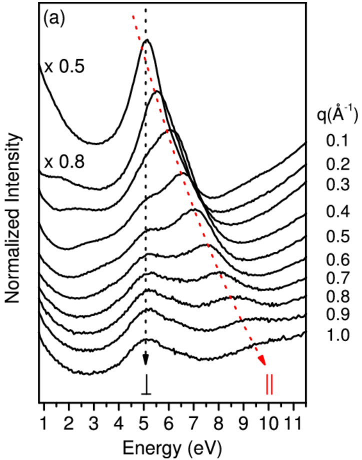

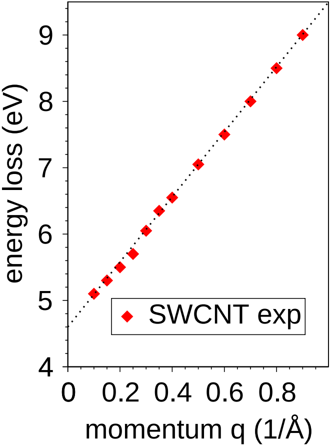

[C. Kramberger, R. H., Ch. Giorgetti, *et.al.*: PRL **101**, 266406 (2008)]

EELS on SWCNTs

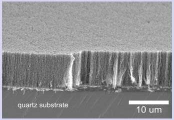

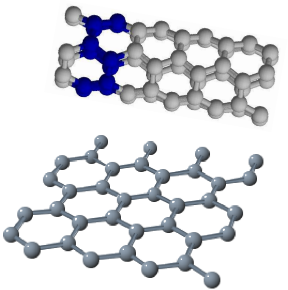

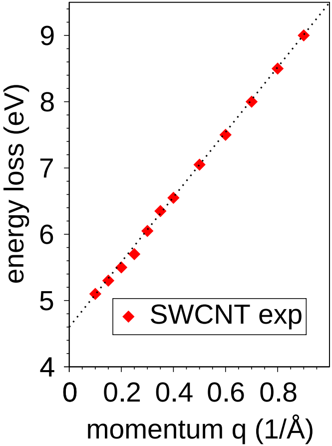

[C. Kramberger, R. H., Ch. Giorgetti, *et.al.*: PRL **101**, 266406 (2008)]

EELS on SWCNTs

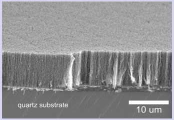

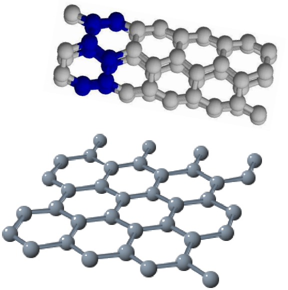

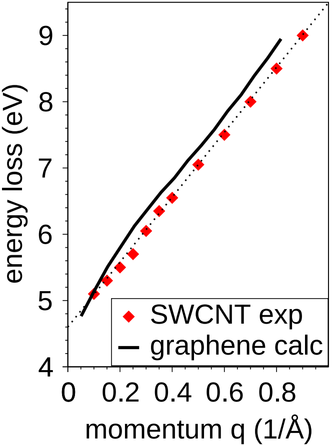

[C. Kramberger, R. H., Ch. Giorgetti, *et.al.*: PRL **101**, 266406 (2008)]

Questions

- on-axis excitations in SWCNTs (ok)
- perpendicular excitations in SWCNTs (?)
- convergence for graphene (?)

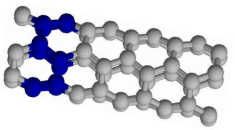

Questions

- on-axis excitations in SWCNTs (ok)
- perpendicular excitations in SWCNTs (?)
- convergence for graphene (?)

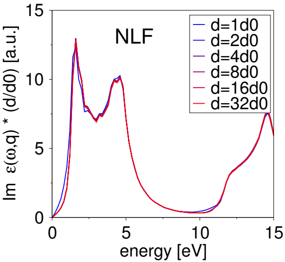

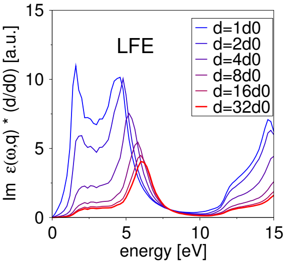

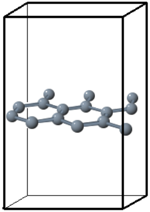

Outline

1. Graphite → Graphene
   - interpolation method
2. Graphene → SWCNTs
   - zone-folding method
3. Local-response approximation
   - connection with dielectric theory

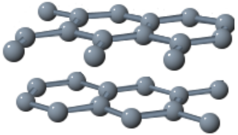

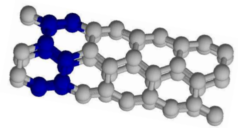

Graphite $\rightarrow$ Graphene

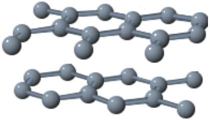

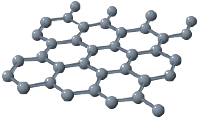

Ab-Initio Calculations for Graphene

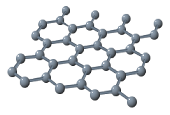

full *ab-initio* calculations

1. ground-state calculation gives ϕ_i^{KS}
2. independent-particle polarisability χ^0
3. susceptibility $\chi = \chi^0 + \chi^0 v \chi$
4. electron energy-loss spectrum
   $S(\boldsymbol{q}, \omega) = -\frac{1}{\pi} \operatorname{Im} \chi(\boldsymbol{qq}, \omega)$

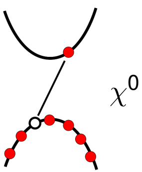

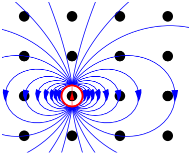

Codes:

ABINIT: X. Gonze *et al.*, Comp. Mat. Sci. **25**, 478 (2002)

DP-code: `www.dp-code.org`; V. Olevano, *et al.*, unpublished.

Ab-Initio Calculations for Graphene

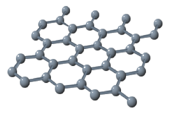

full *ab-initio* calculations

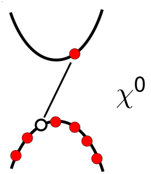

1. ground-state calculation gives ϕ_i^{KS}
2. independent-particle polarisability χ^0
3. susceptibility $\chi = \chi^0 + \chi^0 v \chi$
4. electron energy-loss spectrum
   $S(\boldsymbol{q},\omega) = -\frac{1}{\pi}\,\mathrm{Im}\,\chi(\boldsymbol{qq},\omega)$

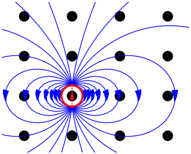

Codes:

ABINIT: X. Gonze *et al.*, Comp. Mat. Sci. **25**, 478 (2002)

DP-code: `www.dp-code.org`; V. Olevano, *et al.*, unpublished.

Polarisability vs Susceptibility

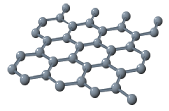

polarisability χ^0 is restricted to sheets and local

$$\chi^0(\boldsymbol{r},\boldsymbol{r}') \propto \sum_{vc} \frac{\varphi_v^*(\boldsymbol{r})\varphi_c(\boldsymbol{r})\varphi_c^*(\boldsymbol{r}')\varphi_v(\boldsymbol{r}')}{\hbar\omega + i\eta - (E_c - E_v)} - \text{a.r.}$$

susceptibility χ is restricted to sheets, but nonlocal

$$\chi(\boldsymbol{r},\boldsymbol{r}') = \chi^0 + \chi^0 v \chi^0 + \chi^0 v \chi^0 v \chi^0 + \dots$$

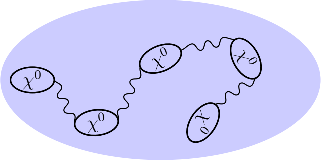

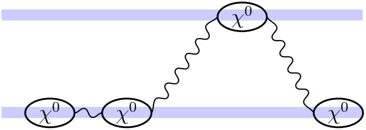

From Graphite to Graphene

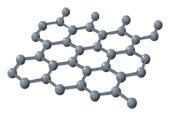

- Coulomb-cutoff method

  C. A. Rozzi *et. al.*, PRB(73) 205119 (2006)
  S. Ismail-Beigi, PRB(73) 233103 (2006)

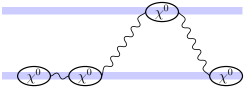

- Interpolation method

Interpolation Method

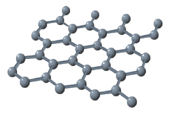

full *ab-initio* for ‘graphite’ ($d = 2 \cdot d_0$)

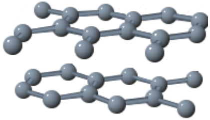

1. ground-state calculation gives ϕ_i^{KS}
2. independent-particle polarisability χ^0_{bulk}

\+ graphite to graphene: $\chi^0_{\mathrm{bulk}} \to \chi^0_{\mathrm{sheet}}$

continue for ‘graphene’ ($d = 2N \cdot d_0$)

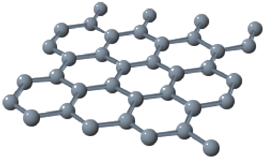

3. susceptibility $\chi = \chi^0_{\mathrm{sheet}} + \chi^0_{\mathrm{sheet}} v \chi$
4. electron energy-loss spectrum
   $S(\boldsymbol{q}, \omega) = -\frac{1}{\pi} \,\mathrm{Im}\, \chi(\boldsymbol{q}\boldsymbol{q}, \omega)$

Interpolation Method

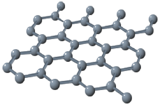

full *ab-initio* for 'graphite' ($d = 2 \cdot d_0$)

1. ground-state calculation gives ϕ_i^{KS}
2. independent-particle polarisability χ^0_{bulk}

\+ graphite to graphene: $\chi^0_{\mathrm{bulk}} \to \chi^0_{\mathrm{sheet}}$

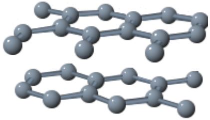

continue for 'graphene' ($d = 2N \cdot d_0$)

3. susceptibility $\chi = \chi^0_{\mathrm{sheet}} + \chi^0_{\mathrm{sheet}} v \chi$
4. electron energy-loss spectrum $S(\boldsymbol{q}, \omega) = -\frac{1}{\pi} \operatorname{Im} \chi(\boldsymbol{qq}, \omega)$

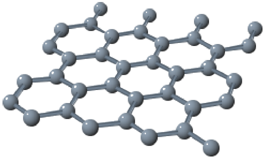

Interpolation Method

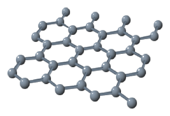

$$\chi^0_{\text{bulk}}(G_z, G'_z) \longrightarrow \chi^0_{\text{bulk}}(z, z') \longrightarrow \chi^0_{\text{sheet}}(z, z') \longrightarrow \chi^0_{\text{sheet}}(G_z, G'_z)$$

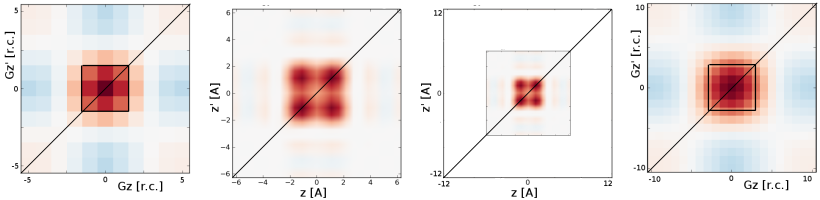

Ab-Initio vs Interpolation

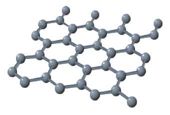

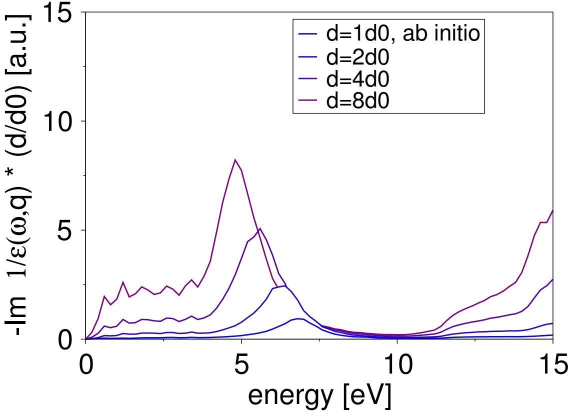

(in-plane momentum transfer $\bar{q} = 0.003\text{Å}^{-1}$)

Ab-Initio vs Interpolation

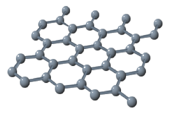

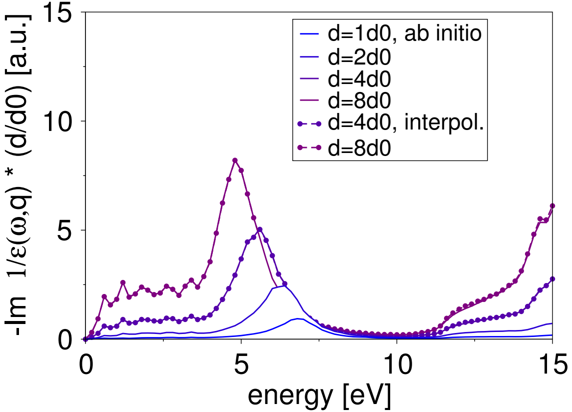

(in-plane momentum transfer $\bar{q} = 0.003\text{Å}^{-1}$)

Ab-Initio vs Interpolation

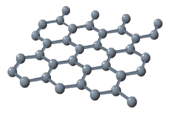

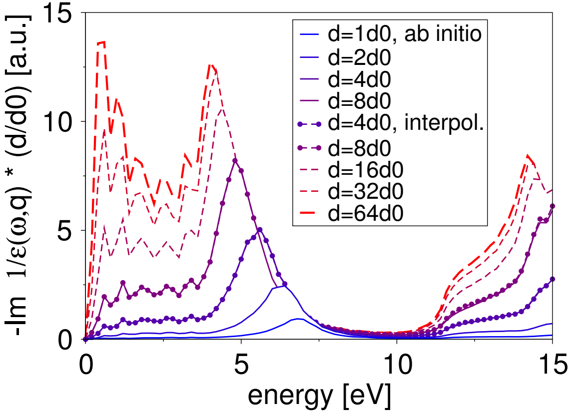

(in-plane momentum transfer $\bar{q} = 0.003\text{Å}^{-1}$)

Summary

- we can avoid calculations with large supercells by interpolation χ^0 in $G_z \longleftrightarrow$ zero-padding in z
- χ^0 is very localized / transferable

Building-Block Approach

- assembly of several layers
- new geometries

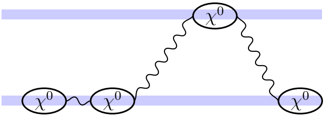

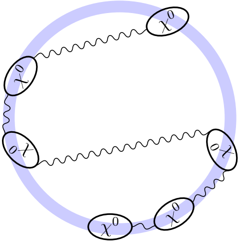

Graphene $\rightarrow$ SWCNT

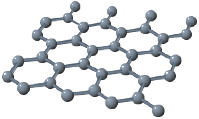

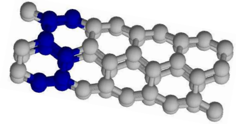

Building-Block Approach for SWCNT

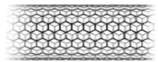

full *ab-initio* for periodic graphene ribbon

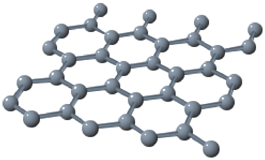

1. ground-state calculation gives ϕ_i^{KS}
2. independent-particle polarisability χ^0_{bulk}

zone-folding model for χ^0

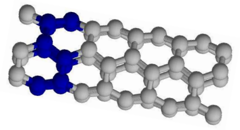

3. polarisability of tube $\chi^0_{\mathrm{bulk}} \to \chi^0_{\mathrm{cnt}}$
4. cylinder susceptibility $\chi = \chi^0_{\mathrm{cnt}} + \chi^0_{\mathrm{cnt}} v \chi$
5. energy-loss $S = -\frac{1}{\pi} \operatorname{Im} \chi(\boldsymbol{qq}, \omega)$

Building-Block Approach for SWCNT

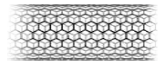

full *ab-initio* for periodic graphene ribbon

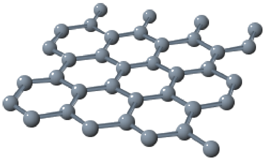

1. ground-state calculation gives ϕ_i^{KS}
2. independent-particle polarisability χ^0_{bulk}

zone-folding model for χ^0

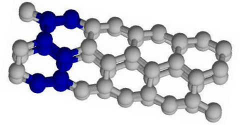

3. polarisability of tube $\chi^0_{\text{bulk}} \to \chi^0_{\text{cnt}}$
4. cylinder susceptibility $\chi = \chi^0_{\text{cnt}} + \chi^0_{\text{cnt}} v \chi$
5. energy-loss $S = -\frac{1}{\pi}\,\text{Im}\,\chi(\boldsymbol{qq},\omega)$

Zone-Folding for Polarisability

real space: cylinder coordinates (ϱ, φ, z)

$$\chi^0(\boldsymbol{\varrho}, \boldsymbol{\varrho}') \cdot \rho' \approx \chi^0_{\text{sheet}}\big(\boldsymbol{r}(\boldsymbol{\varrho}), \boldsymbol{r}(\boldsymbol{\varrho}')\big) \cdot R$$

reciprocal space: helical momentum (m, p)

$$\boxed{\chi^0(mm'pp'; \varrho\varrho', \omega) \cdot \varrho' \approx \chi^0_{\text{sheet}}(q_x q_x', q_y q_y'; zz', \omega)}$$

$m/R \leftrightarrow q_x$	azimuthal momentum
$p \leftrightarrow q_y$	on-axis momentum
$\varrho - R \leftrightarrow z$	radial position

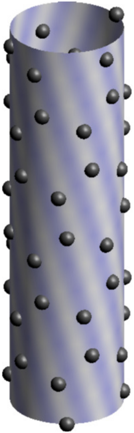

Building-Block Approach for SWCNT

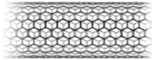

full *ab-initio* for periodic graphene ribbon

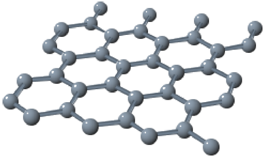

1. ground-state calculation gives ϕ_i^{KS}
2. independent-particle polarisability χ^0_{bulk}

zone-folding model for χ^0

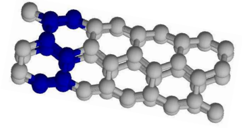

3. polarisability of tube $\chi^0_{\text{bulk}} \to \chi^0_{\text{cnt}}$
4. cylinder susceptibility $\chi = \chi^0_{\text{cnt}} + \chi^0_{\text{cnt}} v \chi$
5. energy-loss $S = -\frac{1}{\pi} \operatorname{Im} \chi(\boldsymbol{qq}, \omega)$

Dyson Equation in Cylindrical Coordinates

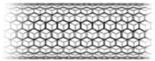

real space:

$$\chi(\boldsymbol{\varrho},\boldsymbol{\varrho}') = \chi^0(\boldsymbol{\varrho},\boldsymbol{\varrho}') + \iint d\boldsymbol{\varrho}_1 d\boldsymbol{\varrho}_2\, \varrho_1 \varrho_2\, \chi^0(\boldsymbol{\varrho},\boldsymbol{\varrho}_1) v(\boldsymbol{\varrho}_1,\boldsymbol{\varrho}_2) \chi(\boldsymbol{\varrho}_2,\boldsymbol{\varrho}')$$

$$v(\boldsymbol{\rho}_1,\boldsymbol{\rho}_2) = \frac{e^2}{4\pi\varepsilon_0} \frac{1}{|\boldsymbol{r}(\boldsymbol{\rho}_1) - \boldsymbol{r}(\boldsymbol{\rho}_2)|}$$

reciprocal space: helical momentum (m,p) [J. D. Jackson]

$$v(m_1 m_2, p_1 p_2; \varrho_1 \varrho_2) = \frac{e^2}{\varepsilon_0} I_{m_1}(|p_1|\rho_<)\, K_{m_1}(|p_1|\rho_>) \delta_{m_1 m_2} \delta(p_1 - p_2)$$

with the modified Bessel-functions of first kind I_m and K_m

$\Longrightarrow$ cylinder susceptibility $\chi(mm', pp', \varrho\varrho')$

Dyson Equation in Cylindrical Coordinates

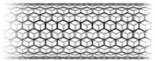

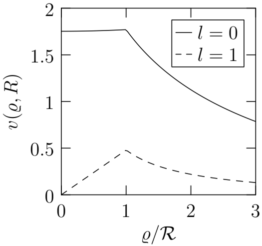

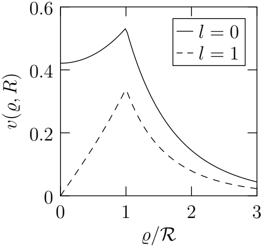

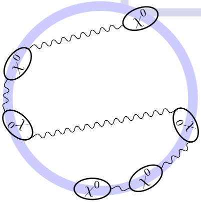

reciprocal space: helical momentum (m, p) [J. D. Jackson]

$$v(m_1 m_2, p_1 p_2; \varrho_1 \varrho_2) = \frac{e^2}{\varepsilon_0} I_{m_1}(|p_1|\rho_<)\, K_{m_1}(|p_1|\rho_>)\delta_{m_1 m_2}\delta(p_1 - p_2)$$

with the modified Bessel-functions of first kind I_m and K_m

$\Longrightarrow$ cylinder susceptibility $\chi(mm', pp', \varrho\varrho')$

Building-Block Approach for SWCNT

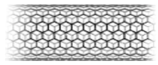

full *ab-initio* for periodic graphene ribbon

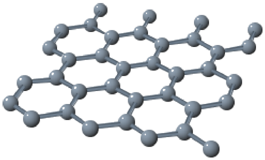

1. ground-state calculation gives ϕ_i^{KS}
2. independent-particle polarisability χ^0_{bulk}

zone-folding model for χ^0

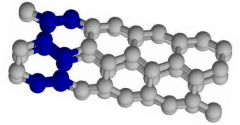

3. polarisability of tube $\chi^0_{\mathrm{bulk}} \rightarrow \chi^0_{\mathrm{cnt}}$
4. cylinder susceptibility $\chi = \chi^0_{\mathrm{cnt}} + \chi^0_{\mathrm{cnt}} v \chi$
5. energy-loss $S = -\frac{1}{\pi}\,\mathrm{Im}\,\chi(\boldsymbol{qq}, \omega)$

AR-EELS for a SWCNT

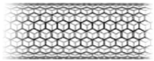

- expand external pert. in cylinder waves, $\boldsymbol{q} = (\boldsymbol{q}_\perp, p)$:

$$e^{i\boldsymbol{qr}} = e^{iq_\perp \varrho \cos\varphi} e^{ipz} = \sum_m i^m J_m(|\boldsymbol{q}_\perp|\varrho)\; e^{im\varphi} e^{ipz}$$

- susceptibility in Cartesian coord.

$$\chi(\boldsymbol{qq}) \approx \frac{2\pi}{L^2} \sum_{m,m'} \iint d\varrho d\varrho'\; \varrho\varrho' (-i)^{m-m'} \cdot$$
$$\cdot J_m(|\boldsymbol{q}_\perp|\varrho) J_{m'}(|\boldsymbol{q}_\perp|\varrho') \chi(mm', pp, \varrho\varrho')$$

- energy-loss function

$$S(\boldsymbol{q}, \omega) = -\tfrac{1}{\pi} \operatorname{Im} \chi(\boldsymbol{qq}, \omega)$$

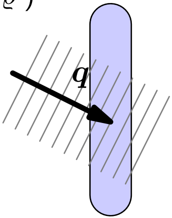

AR-EELS for a SWCNT

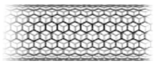

- expand external pert. in cylinder waves, $\boldsymbol{q} = (\boldsymbol{q}_\perp, p)$:

$$e^{i\boldsymbol{q}\boldsymbol{r}} = e^{iq_\perp \varrho \cos\varphi} e^{ipz} = \sum_m i^m J_m(|\boldsymbol{q}_\perp|\varrho)\; e^{im\varphi} e^{ipz}$$

- susceptibility in Cartesian coord.

$$\chi(\boldsymbol{q}\boldsymbol{q}) \approx \frac{2\pi}{L^2} \sum_{m,m'} \iint d\varrho d\varrho'\; \varrho\varrho'(-i)^{m-m'} \cdot$$

$$\cdot J_m(|\boldsymbol{q}_\perp|\varrho) J_{m'}(|\boldsymbol{q}_\perp|\varrho') \chi(mm', pp, \varrho\varrho')$$

- energy-loss function

$$S(\boldsymbol{q}, \omega) = -\frac{1}{\pi} \operatorname{Im} \chi(\boldsymbol{q}\boldsymbol{q}, \omega)$$

$\Longrightarrow$ numerical test for CNT(9,9)

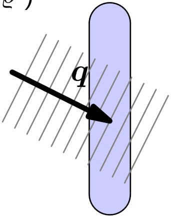

Ab-Initio vs. Zone-Folding: CNT(9,9)

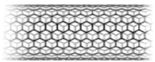

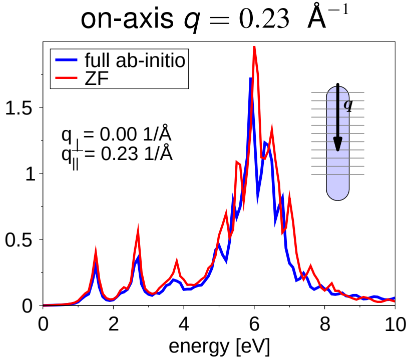

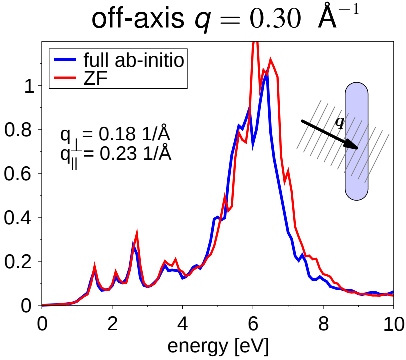

Ab-Initio vs. Zone-Folding: CNT(9,9)

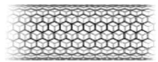

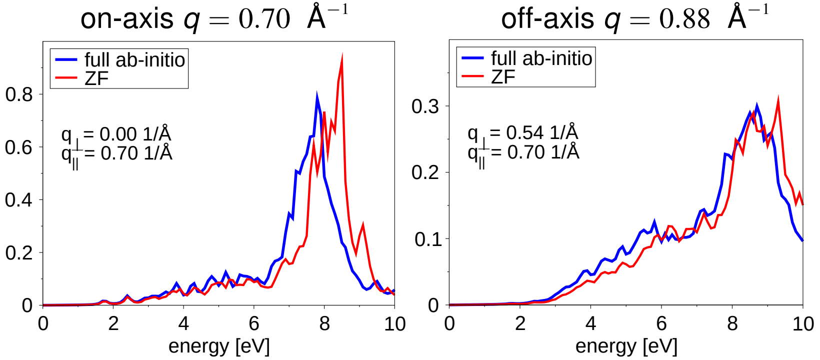

Summary

- zone-folding: graphene $\rightarrow$ SWCNT
- computational effort reduced (two-atom unit cell)
- microscopic dielectric theory for $\epsilon(\boldsymbol{q}\boldsymbol{q}', \omega)$

Local-Response Approximation

- connection with local dielectric theory $\epsilon_{\mathrm{M}}(\boldsymbol{q}, \omega)$
- analytic solution for Dyson equation $\chi = \chi^0 + \chi^0 v \chi$
- interpretation in terms of normal mode excitations

Local-Response Approximation

connection with dielectric theory

Dyson Equation in Cylindrical Coordinates

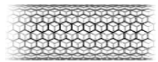

Dyson equation: coordinates (m, p, ϱ)

$$\chi(\varrho,\varrho') = \chi^0(\varrho,\varrho') + \iint d\varrho_1 d\varrho_2\, \varrho_1 \varrho_2\, \chi^0(\varrho,\varrho_1) v(\varrho_1,\varrho_2) \chi(\varrho_2,\varrho')$$

$$v(m,p;\varrho_1\varrho_2) = \frac{e^2}{\varepsilon_0} I_m(|p|\rho_<)\, K_m(|p|\rho_>)$$

$p = 0.2/R$

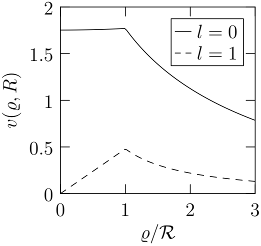

$p = 1/R$

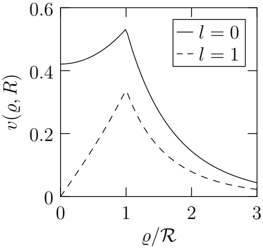

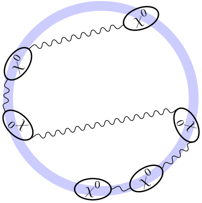

Dyson Equation in Cylindrical Coordinates

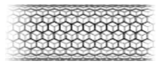

Dyson equation: coordinates (m, p, ϱ)

$$\chi(\varrho,\varrho') = \chi^0(\varrho,\varrho') + \iint d\varrho_1 d\varrho_2\, \varrho_1 \varrho_2\, \chi^0(\varrho,\varrho_1)\, v(R\,,R\,)\, \chi(\varrho_2,\varrho')$$

$$v(m,p;R,R) = \frac{e^2}{\varepsilon_0} I_m(|p|R)\, K_m(|p|R) \equiv v_{\mathrm{cnt}}(m,p)$$

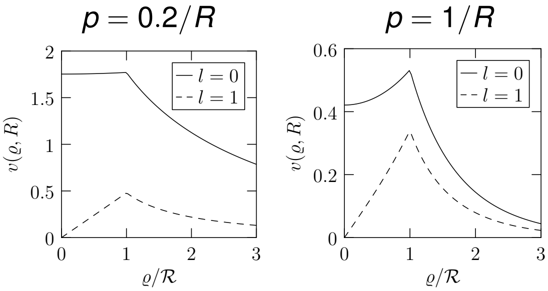

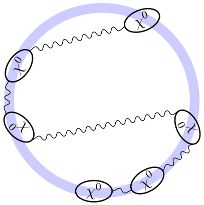

Dyson Equation in Cylindrical Coordinates

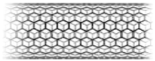

Dyson equation: coordinates (m, p, ϱ)

$$\chi(\varrho, \varrho') = \chi^0(\varrho, \varrho') + \iint d\varrho_1 d\varrho_2\, \varrho_1 \varrho_2\, \chi^0(\varrho, \varrho_1) v(R, R) \chi(\varrho_2, \varrho')$$

$$v(m, p; R, R) = \frac{e^2}{\varepsilon_0} I_m(|p|R)\, K_m(|p|R) \equiv v_{\text{cnt}}(m, p)$$

integrated cylinder response functions

$$\bar{\chi}^0(m, p) \equiv \iint d\rho_1 d\rho_2\, \rho_1 \rho_2\, \chi^0(mm, pp; \rho_1 \rho_2)$$

scalar Dyson equation

$$\boxed{\bar{\chi}(m, p) \approx \bar{\chi}^0(m, p) + \bar{\chi}^0(m, p)\, v_{\text{cnt}}(m, p)\, \bar{\chi}(m, p)}$$

[M. F. Lin, *et al.*: PRB, 53, 15493 (1996).]

Local-Response Approximation

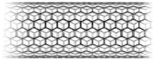

full *ab-initio* for periodic graphene ribbon

1. ground-state calculation gives ϕ_i^{KS}
2. independent-particle polarisability χ^0_{bulk}

zone-folding model for χ^0

3. polarisability of tube $\bar{\chi}^0(m,p) = R \cdot \chi^0_{\mathrm{bulk}}(q_x, q_y)$
4. cylinder susceptibility $\bar{\chi} \approx \bar{\chi}^0 + \bar{\chi}^0 v_{\mathrm{cnt}} \bar{\chi}$
5. energy-loss $\chi(\boldsymbol{qq}, \omega) \approx \frac{2\pi}{L^2} \sum_m J_m^2(|\boldsymbol{q}_\perp| R)\ \bar{\chi}(m,p)$

Local-Response Approximation

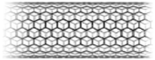

Local limit: assume $v(m,p;\varrho_1,\varrho_2) \approx v(m,p;R,R)$

- neglect in-plane crystal local-field effects
- only valid if both m and p are small

zone-folding model for χ^0

3. polarisability of tube $\bar{\chi}^0(m,p) = R \cdot \chi^0_{\text{bulk}}(q_x, q_y)$
4. cylinder susceptibility $\bar{\chi} \approx \bar{\chi}^0 + \bar{\chi}^0 v_{\text{cnt}} \bar{\chi}$
5. energy-loss $\chi(\boldsymbol{qq},\omega) \approx \frac{2\pi}{L^2} \sum_m J_m^2(|\boldsymbol{q}_\perp|R)\, \bar{\chi}(m,p)$

Local-Response Approximation

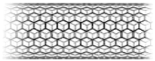

Local limit: assume $v(m,p;\varrho_1,\varrho_2) \approx v(m,p;R,R)$

- neglect in-plane crystal local-field effects
- only valid if both m and p are small

zone-folding model for χ^0

3. polarisability of tube $\bar{\chi}^0(m,p) = R \cdot \chi^0_{\text{bulk}}(q_x,q_y)$
4. cylinder susceptibility $\bar{\chi} \approx \bar{\chi}^0 + \bar{\chi}^0 v_{\text{cnt}} \bar{\chi}$
5. energy-loss $\chi(\boldsymbol{q}\boldsymbol{q},\omega) \approx \frac{2\pi}{L^2} \sum_m J_m^2(|\boldsymbol{q}_\perp|R)\, \bar{\chi}(m,p)$

Cylinder Response for CNT(9,9)

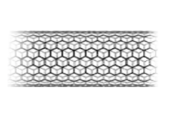

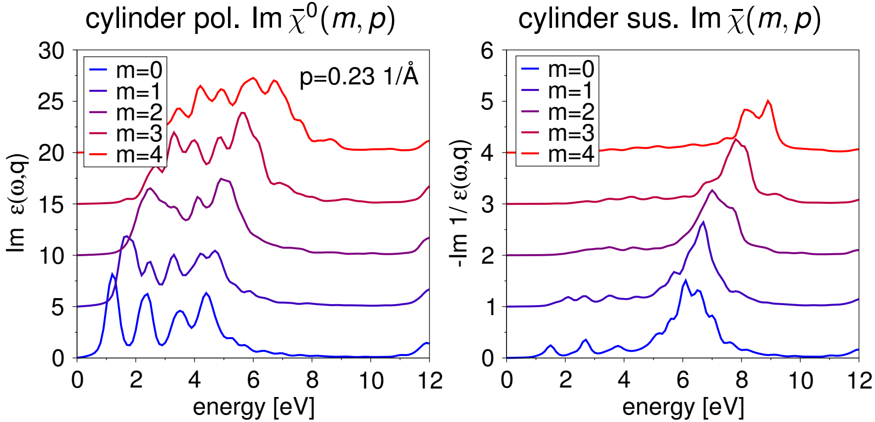

Local-Response Approximation

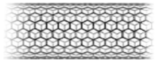

Local limit: assume $v(m,p;\varrho_1,\varrho_2) \approx v(m,p;R,R)$

- neglect in-plane crystal local-field effects
- only valid if both m and p are small

zone-folding model for χ^0

3. polarisability of tube $\bar{\chi}^0(m,p) = R \cdot \chi^0_{\mathrm{bulk}}(q_x,q_y)$
4. cylinder susceptibility $\bar{\chi} \approx \bar{\chi}^0 + \bar{\chi}^0 v_{\mathrm{cnt}} \bar{\chi}$
5. energy-loss $\chi(\boldsymbol{q}\boldsymbol{q},\omega) \approx \frac{2\pi}{L^2} \sum_m J_m^2(|\boldsymbol{q}_\perp| R)\, \bar{\chi}(m,p)$

AR-EELS for CNT(9,9): small q

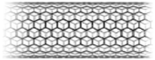

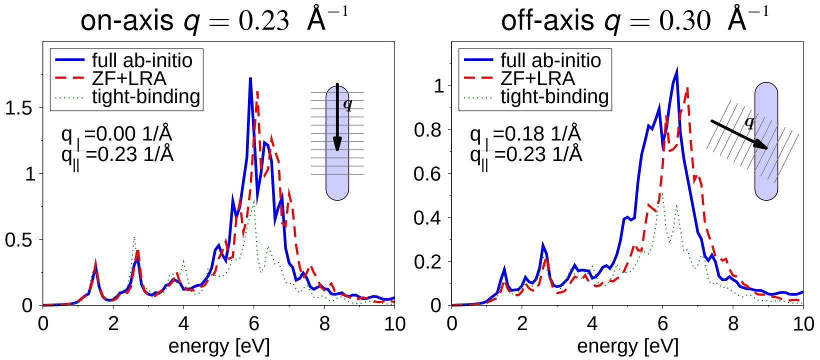

m	0	± 1	± 2	± 3
J_m^2	1	0	0	0

m	0	± 1	± 2	± 3
J_m^2	0.5	0.2	0	0

AR-EELS for CNT(9,9): large q

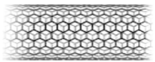

on-axis $q = 0.70$ Å^{-1}

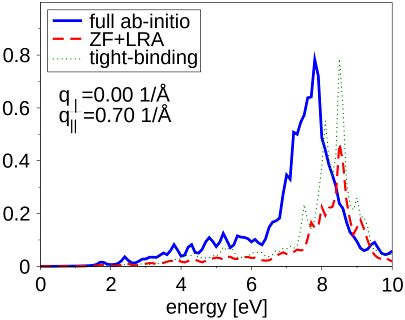

off-axis $q = 0.88$ Å^{-1}

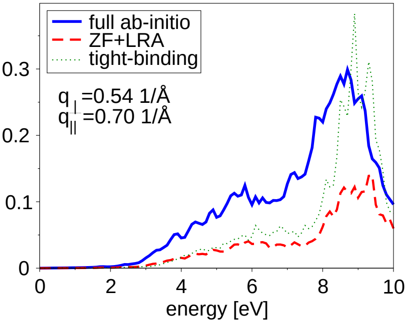

m	0	±1	±2	±3
J_m^2	1	0	0	0

m	0	±1	±2	±3
J_m^2	0.1	0.05	0.2	0.1

AR-Experiments vs. Tight-Binding

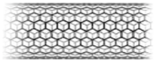

Experiment: oriented SWCNT
(Diameter 20 Å, nearly isolated)

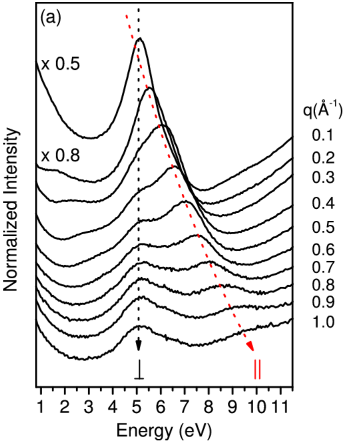

TB-Calculation: (9,9) SWCNT
($|q| = 0.4$Å varying orientation)

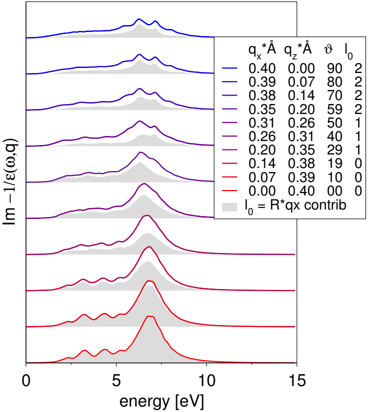

Summary

- introduced effective, scalar response functions
- dyson equation can be solved analytically
- AR-EELS in terms of normal-mode excitations
- approximation holds for small $|\boldsymbol{q}| < 0.1$ Å

Outlook

- effects on tubes: chirality, diameter, orientation
- exchange-correlation effects
- different perturbation: spatially-resolved EELS

Conclusions

1. Graphite → Graphene
   - interpolation method
2. Graphene → SWCNTs
   - zone-folding method
3. Local-response approximation
   - connection with dielectric theory
   - analysis using normal modes

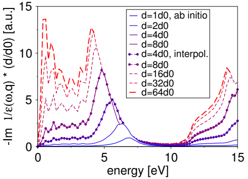

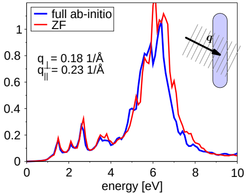

$$\bar{\chi} \approx \bar{\chi}^0 + \bar{\chi}^0 v_{\text{cnt}} \bar{\chi}$$

Appendix

Tight-Binding for CNT(9,9)

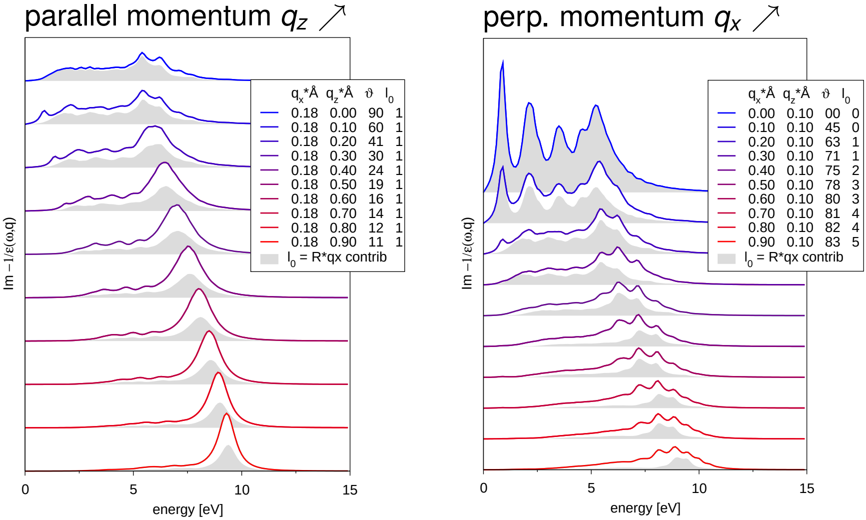

Tight-Binding for (3,3) Nanotube

Calculation: (3,3) SWCNT
(Diameter 4 Å, low interaction)

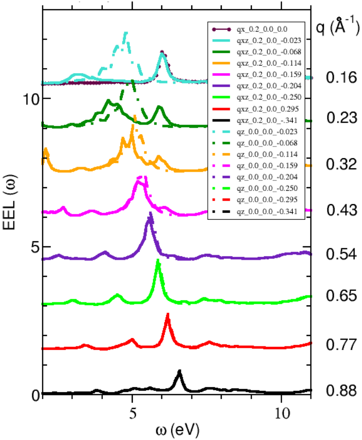

TB-Calculation: (3,3) SWCNT
($|q_x| = 0.18$Å, $q_z \nearrow$)

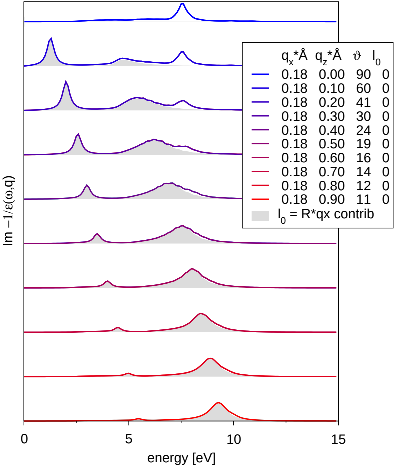

Example: CNT(9,9)

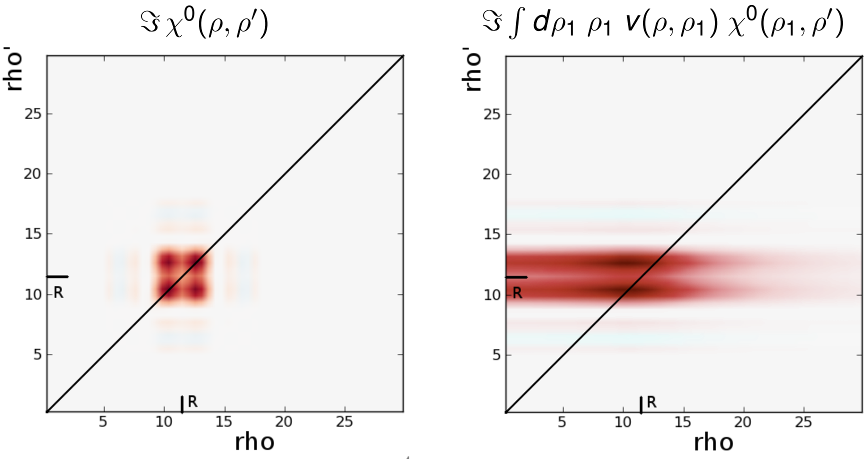

(CNT(9,9), $q_z = q'_z = 0.27\text{Å}^{-1}, m = m' = 0, \omega = 4\text{eV}$)

Dielectric Theory

local dielectric function:

$$\epsilon(\omega) = 1 + v\chi^0(\omega)$$

including nonlocal effects:

$$\epsilon(\boldsymbol{q},\omega) = 1 + v(\boldsymbol{q})\chi^0(\boldsymbol{q},\omega)$$

microscopic dielectric theory:

$$\epsilon(\boldsymbol{q}\boldsymbol{q}',\omega) = \delta(\boldsymbol{q}-\boldsymbol{q}')+v(\boldsymbol{q})\chi^0(\boldsymbol{q}\boldsymbol{q}',$$

[Stöckli, Phil. Mag. B (79), 1531 (1999)]

Planar graphite:

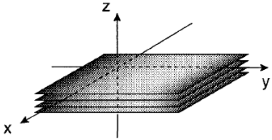

Carbon nanotube:

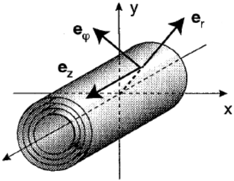

3D Dyson Equation

real space

$$\chi(\boldsymbol{r},\boldsymbol{r}') = \chi^0(\boldsymbol{r},\boldsymbol{r}') + \iint d\boldsymbol{r}_1 d\boldsymbol{r}_2\ \chi^0(\boldsymbol{r},\boldsymbol{r}_1) v(\boldsymbol{r}_1,\boldsymbol{r}_2)\chi(\boldsymbol{r}_2,\boldsymbol{r}')$$

$$v(\boldsymbol{r}_1,\boldsymbol{r}_2) = \frac{e^2}{4\pi\varepsilon_0}\frac{1}{|\boldsymbol{r}_1-\boldsymbol{r}_2|}$$

reciprocal space

$$v(\boldsymbol{q}_1,\boldsymbol{q}_2) = v_{3D}(q_1)\ \delta(\boldsymbol{q}_1-\boldsymbol{q}_2), \qquad v_{3D} \equiv \frac{e^2}{\varepsilon_0}\frac{1}{q^2}$$

$$v(\bar{\boldsymbol{q}}_1 z_1,\bar{\boldsymbol{q}}_2 z_2) = v_{2D}(q_1)\ e^{-|\bar{q}||z_1-z_2|}\ \delta(\bar{\boldsymbol{q}}_1-\bar{\boldsymbol{q}}_2), \quad v_{2D} \equiv \frac{e^2}{2\varepsilon_0}\frac{1}{\bar{q}}$$

2D Dyson Equation

Local Response Approximation (1)

We let $e^{-|\bar{q}_1||z_1-z_2|} \approx 1$ for $\bar{q}_1 \ll \frac{1}{2\lambda} \approx 0.5\,\text{Å}^{-1}$ due to the locality of $\chi^{(0)}$. Introducing the integrated (2D) quantities

$$\bar{\chi}^{(0)}(\bar{\boldsymbol{q}}_1, \bar{\boldsymbol{q}}_2) \equiv \iint dz_1 dz_2\, \chi^{(0)}(\bar{\boldsymbol{q}}_1 z_1, \bar{\boldsymbol{q}}_2 z_2)$$

we find the (2D) Dyson Equation

$$\bar{\chi} = \bar{\chi}^0 + \bar{\chi}^0 v_{2D} \bar{\chi}, \qquad \bar{\epsilon} = 1 - v_{2D} \bar{\chi}^0$$

LRA vs Ab-Initio

Ab-Initio calculation

- Graphene LF-spectrum
  $\bar{\chi} = d \cdot \chi(\bar{\boldsymbol{q}}\bar{\boldsymbol{q}}, q_z = 0)$

Calculation using LRA + neglecting in-plane LFE

- Graphite NLF-spectrum
  $\bar{\chi}^0 = d_0 \cdot \chi^0(\bar{\boldsymbol{q}}\bar{\boldsymbol{q}}, q_z = 0)$
- 2D Dyson equation
  $\bar{\chi} = \bar{\chi}^0 + \bar{\chi}^0 v_{2D} \bar{\chi}$

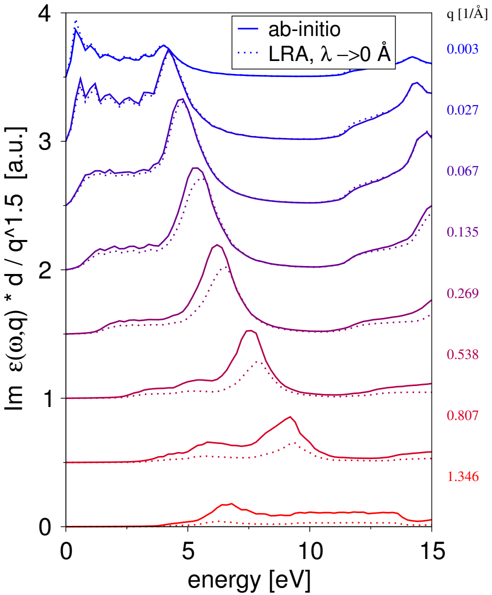

2D Dyson Equation

Local Response Approximation (2)

We assume separability and an exponential decay in z and z' $\chi^{(0)}(\bar{\boldsymbol{q}}, zz') = e^{-(|z|+|z'|)/\lambda}\, \chi^{(0)}(\bar{\boldsymbol{q}})$. By integrating

$$\chi^0 v \chi = \int dz_1 dz_2 d\bar{\boldsymbol{q}}_1\ \chi^0(\bar{\boldsymbol{q}}z, \bar{\boldsymbol{q}}_1 z_1)\ v_{2D}\, e^{-|\bar{q}_1||z_1-z_2|}\ \chi(\bar{\boldsymbol{q}}_1 z_2, \bar{\boldsymbol{q}}' z')$$

we find the (2D) Dyson Equation

$$\bar{\chi}^\lambda = \bar{\chi}^0 + \bar{\chi}^0\ \frac{v_{2D}}{\beta_\lambda}\ \bar{\chi}^\lambda, \qquad \beta_\lambda = \frac{(1+|\bar{q}|\lambda)^2}{1+\frac{1}{2}|\bar{q}|\lambda} \approx 1 + \tfrac{3}{2}|\bar{q}|\lambda + \dots$$

LRA-λ vs Ab-Initio

Ab-Initio calculation

- Graphene LF-spectrum
  $\bar{\chi} = d \cdot \chi(\bar{\boldsymbol{q}}\bar{\boldsymbol{q}}, q_z = 0)$

Calculation using LRA-λ + neglecting in-plane LFE

- Graphite NLF-spectrum
  $\bar{\chi}^0 = d_0 \cdot \chi^0(\bar{\boldsymbol{q}}\bar{\boldsymbol{q}}, q_z = 0)$
- 2D Dyson eq, $\lambda = 1.5$Å
  $\bar{\chi}^\lambda = \bar{\chi}^0 + \bar{\chi}^0 \frac{v_{2D}}{\beta_\lambda} \bar{\chi}^\lambda$